Supporting Information

Enabling High-Areal-Capacity Lithium-Sulfur Batteries: Designing Anisotropic and Low-Tortuosity Porous Architectures

Yiju Li[1, a], Kun (Kelvin) Fu[1, a], Chaoji Chen[1], Wei Luo[1], Tingting Gao[1], Shaomao Xu[1], Jiaqi Dai[1], Glenn Pastel[1], Yanbin Wang[1], Boyang Liu[1], Jianwei Song[1], Yanan Chen[1], Chunpeng Yang[1], Liangbing Hu[1,*]

[1] Department of Materials Science and Engineering, University of Maryland College Park, College Park, Maryland, 20742, USA

[*] Email: binghu@umd.edu

[a] These authors contributed equally to this work.

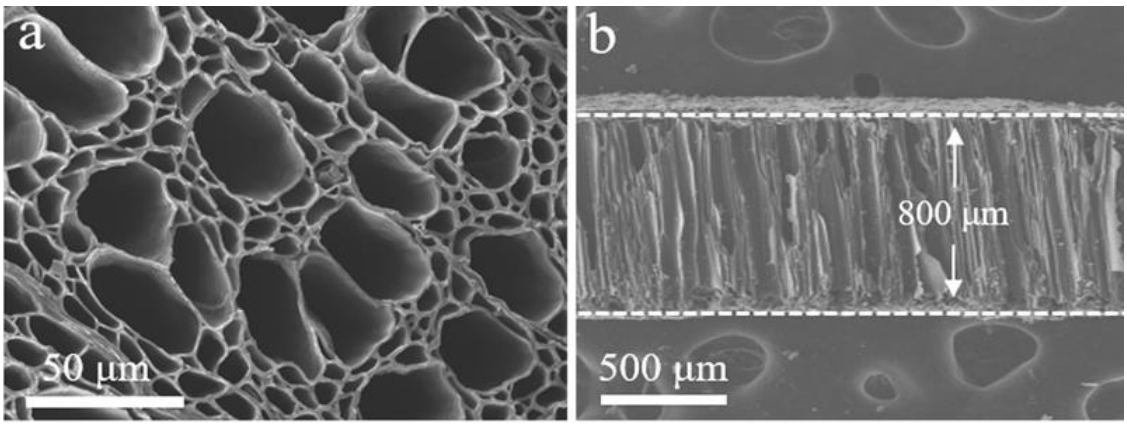

Figure S1. (a) SEM image of the top surface of the bare wood carbon. (b) SEM image shows the thickness of the typical bare wood carbon. The elongated and low-tortuosity microchannels can effectively confine electrolyte and contribute to fast Li-ion transport.

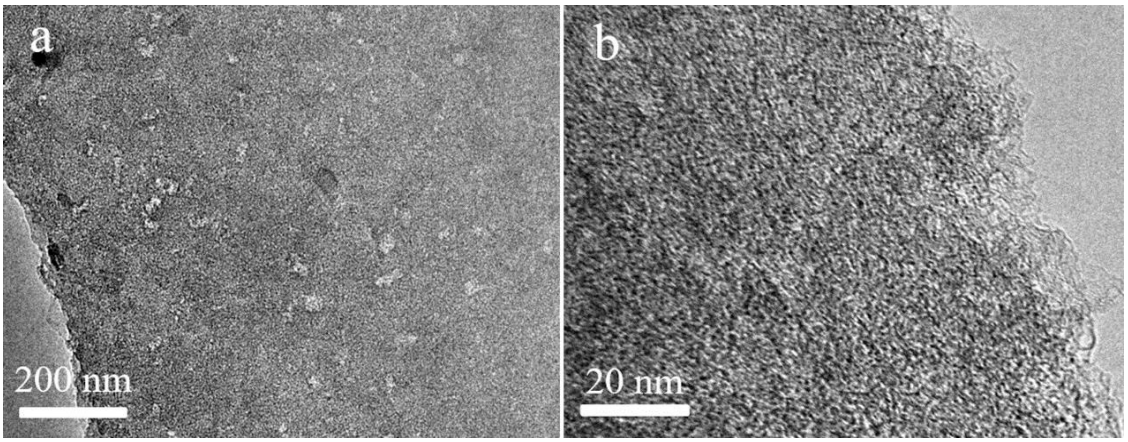

Figure S2. TEM images of bare wood carbon showing numerous hierarchical nanopores on the wall of microchannels.

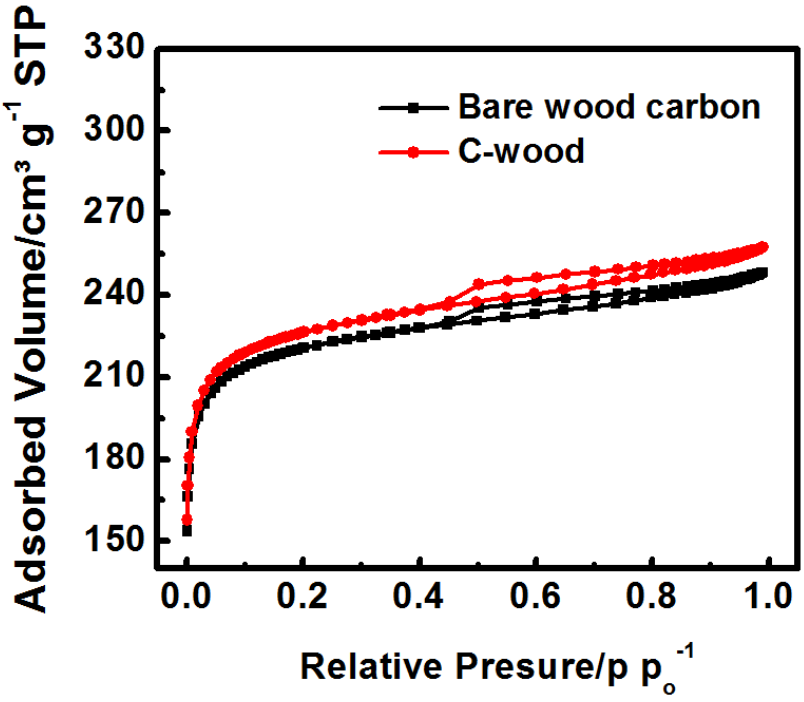

Figure S3. N_2 adsorption-desorption isotherm curves of the bare wood carbon and C-wood.

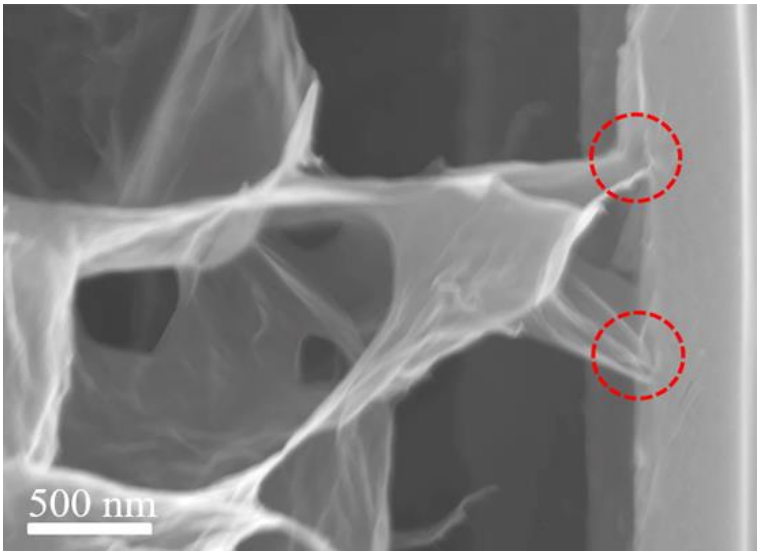

Figure S4. SEM image of the C-wood composite, which shows the tight bond between the wall of bare wood carbon and the RGO nanosheets. The joint enables electron transport between the wall of microchannels and the RGO networks.

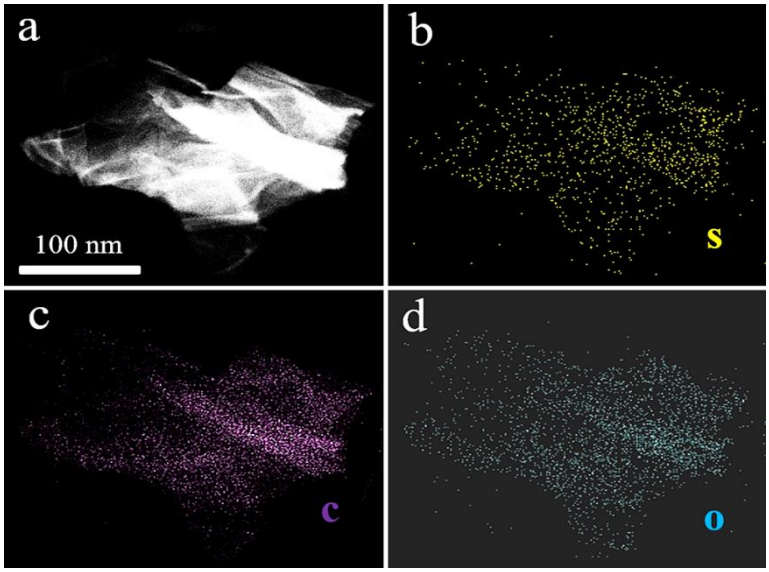

Figure S5. TEM image and corresponding elemental mappings of single RGO nanosheet loaded with sulfur, which displays uniform sulfur distribution on RGO nanosheet.

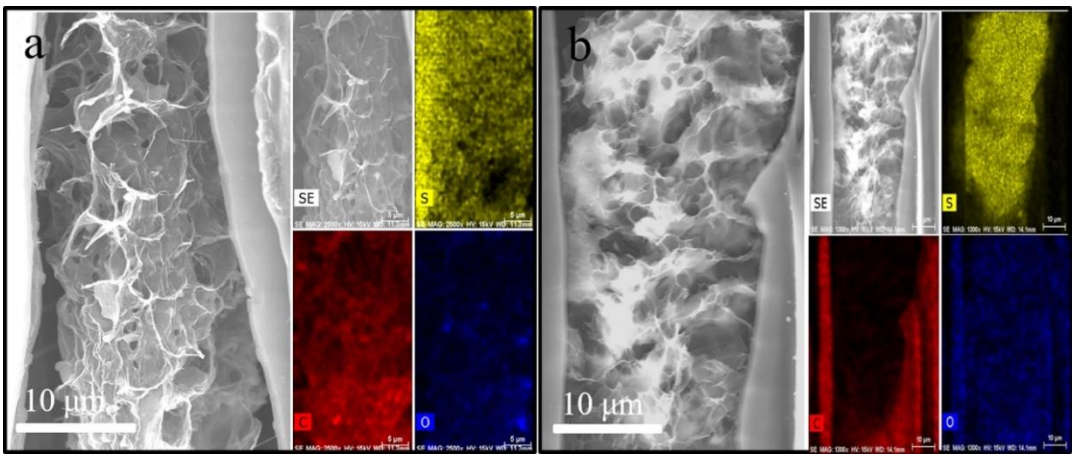

Figure S6. SEM images and corresponding elemental mappings of the S@C-wood composites with sulfur mass loadings of 15.2 mg cm^{-2} (a) and 21.3 mg cm^{-2} (b), respectively.

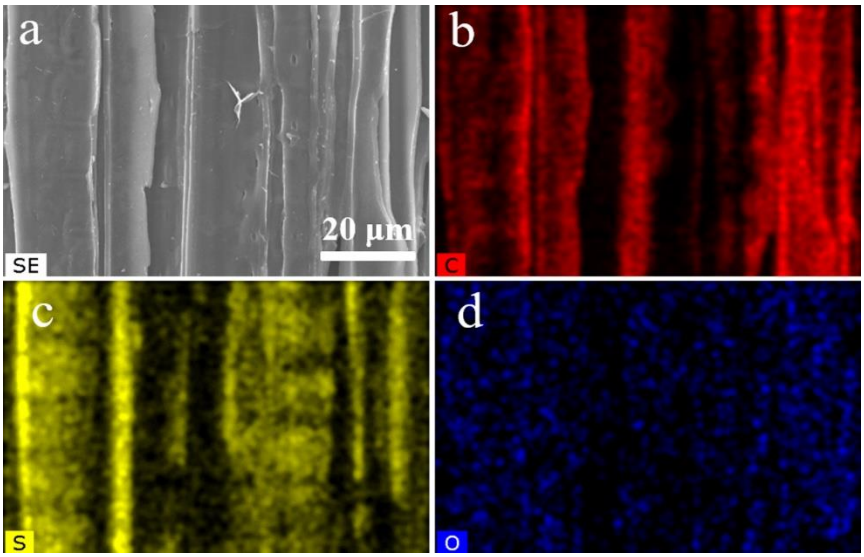

Figure S7. SEM image and corresponding elemental mappings of the S@bare wood carbon composite. The sulfur is uniformly dispersed on the surface inside the aligned microchannels.

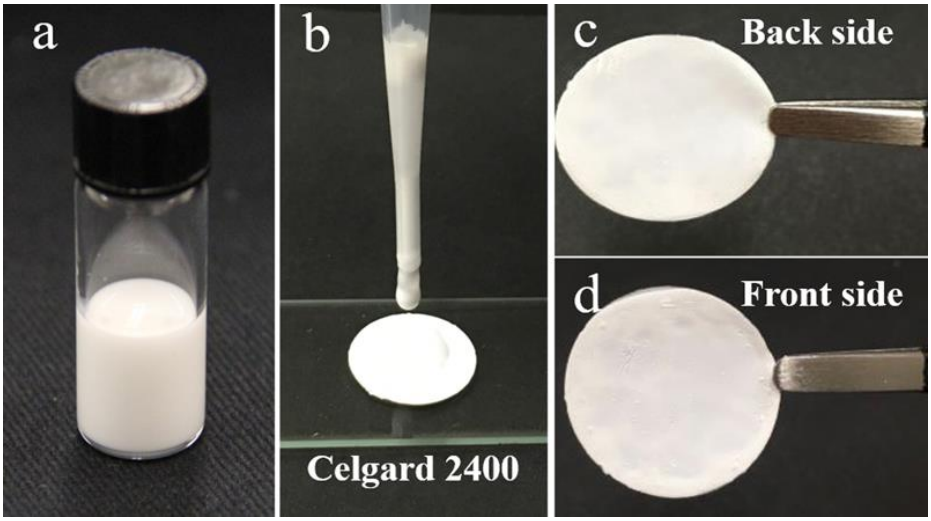

Figure S8. Photographs of the fabrication process of PEO gel composite membrane. (a) Photograph of homogenous PEO gel composite solution. (b) Photograph of dropping PEO gel composite electrolyte onto Celgard 2400. (c, d) Photographs of the back side and front side of the PEO gel composite membrane.

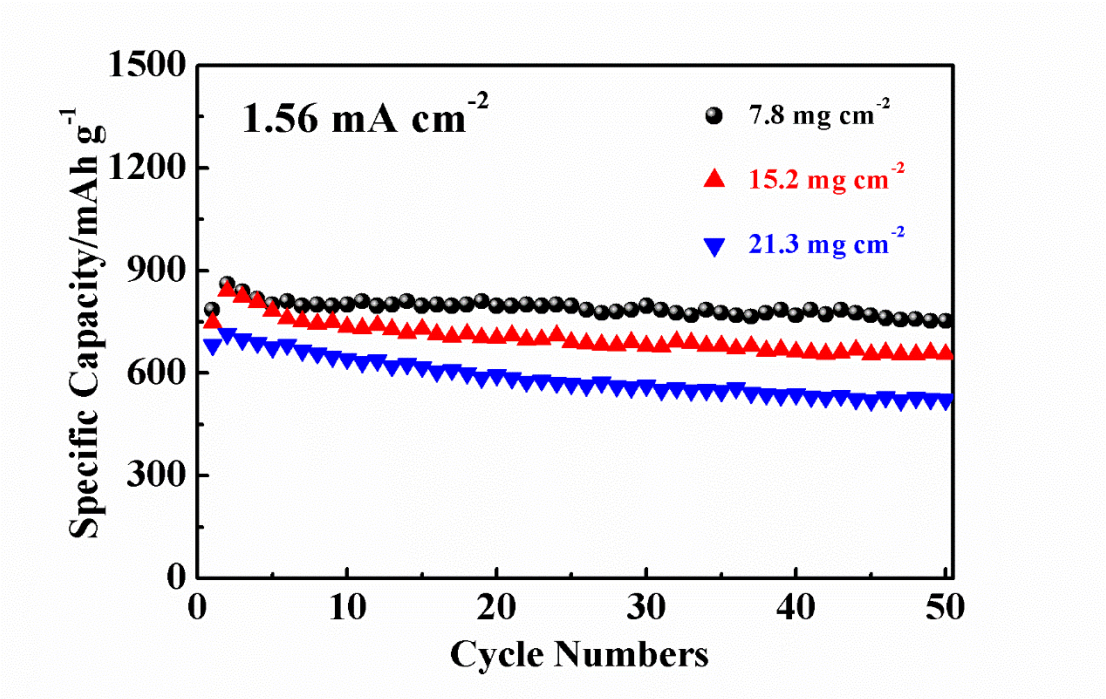

Figure S9. Cycling performance of the S@C-wood composite electrodes with different sulfur mass loadings.

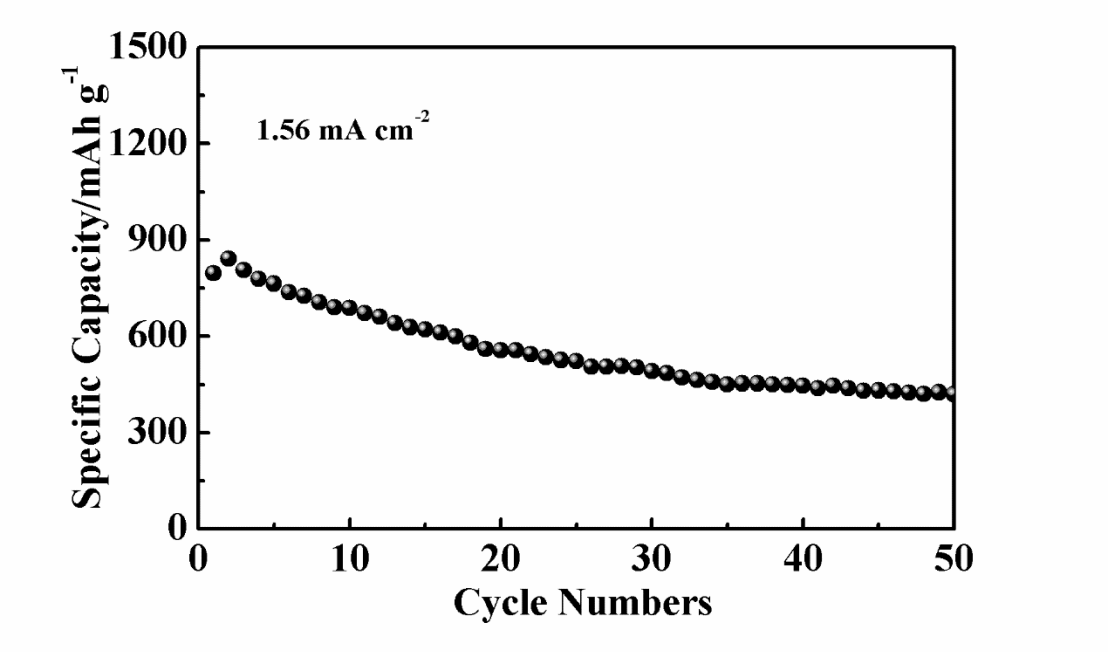

Figure S10. Cycling performance of S@bare wood carbon electrode with a sulfur mass loading of 7.8 mg cm^{-2}. Rapid decay of specific capacity indicates the poor cycling stability of S@bare wood carbon electrode, which confirms the role of RGO in our design for achieving excellent cycling stability.